Tetrahedron 66 (2010) 5594–5601

Contents lists available at ScienceDirect

Tetrahedron

journal homepage: www.elsevier.com/locate/tet

Fluorescence properties of polyamines bearing two terminal quinoline fragments in water

Chizuru Ichimura, Yasuhiro Shiraishi *, Takayuki Hirai

Research Center for Solar Energy Chemistry, and Division of Chemical Engineering, Graduate School of Engineering Science, Osaka University, Toyonaka 560-8531, Japan

ARTICLE INFO

Article history:
Received 26 March 2010
Received in revised form 22 May 2010
Accepted 24 May 2010
Available online 31 May 2010

Keywords:
Quinoline
Polyamine
Zinc(II)
Fluorescent probe
Water

ABSTRACT

Fluorescence properties of polyamines bearing two terminal quinoline fragments with different polyamine chain length, such as ethylenediamine (**L0**), diethylenetriamine (**L1**), and triethylenetetramine (**L2**), have been studied in water. These ligands show Zn^{2+}-induced fluorescence enhancement, while showing almost no enhancement with other cations. However, stability constants for Zn^{2+} coordination and fluorescence response against Zn^{2+} depend strongly on the polyamine chain length. The chain length also affects the fluorescence wavelength. The Zn^{2+}–**L1** and Zn^{2+}–**L2** complexes show emission at 410 nm, while Zn^{2+}–**L0** complexes show a blue-shifted emission at 375 nm due to the partial charge transfer from the excited state quinoline to the Zn^{2+} center.

1. Introduction

Zn(II) is an essential nutrient for human body and plays important roles in many physiological and pathological processes.[1] Design of fluorescent Zn^{2+} probes has therefore attracted a great deal of attention because they allow rapid Zn^{2+} monitoring by simple fluorescence analysis.[2] Various fluorescent Zn^{2+} probes have been proposed so far based on several fluorophores, such as fluorescein,[3] coumarin,[4] dansylamide,[5] and BODIPY.[6] In particular, quinoline-based Zn^{2+} probes have attracted much attention because the quinoline moieties also behave as a ligand for Zn^{2+} coordination.[7] Many of Zn^{2+} probes, however, suffer from several problems: (i) low solubility in water,[8] (ii) strong background fluorescence even without Zn^{2+},[6a,b,7c,9] and (iii) nonstoichiometrical response to Zn^{2+} amount.[3e,6a,c] There are only a few reports of water-soluble fluorescent Zn^{2+} probes capable of covering these issues.[10]

Earlier, we reported a simple quinoline-based ligand, **L1**, consisting of a diethylenetriamine chain and two terminal quinoline moieties (Scheme 1), that behaves as a fluorescent Zn^{2+} probe capable of overcoming these issues.[11] **L1** has a good solubility in water (up to 1 mM) and shows almost no background fluorescence. Addition of Zn^{2+}, however, creates a large fluorescence enhancement, whereas, other metal cations do not. The **L1** fluorescence shows a linear and stoichiometrical response to the Zn^{2+} amount and, hence, allows quantitative Zn^{2+} detection in aqueous media. The probe still involves some problems, such as relatively low fluorescence quantum yield (3–4%) and the need of UV light as an excitation light. However, the above advantages provide important information for the development of more efficient water-soluble Zn^{2+} probes.

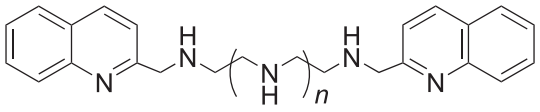

L0 $n = 0$
L1 $n = 1$
L2 $n = 2$

Scheme 1. Structure of ligands.

The purpose of the present work is to further clarify the properties of quinoline–polyamine conjugate as a Zn^{2+} probe. In this work, effects of polyamine chain length on the fluorescence properties have been studied. We synthesized two kinds of ligands with different chain lengths, such as ethylenediamine (**L0**) and triethylenetetramine (**L2**) (Scheme 1). The fluorescence properties of these ligands were compared with that of **L1**. These ligands display high water solubility, no background fluorescence, and Zn^{2+}-induced fluorescence enhancement, as does **L1**. The fluorescence properties of these ligands, however, strongly depend on the chain length in respect to coordination strength, quantitative capability, Zn^{2+} selectivity, and emission wavelength. We describe

* Corresponding author. Tel.: +81 6 6850 6271; fax: +81 6 6850 6273; e-mail address: shiraish@cheng.es.osaka-u.ac.jp (Y. Shiraishi).

0040-4020/$ – see front matter © 2010 Elsevier Ltd. All rights reserved.
doi:10.1016/j.tet.2010.05.096

here the detailed coordination and fluorescence properties of the ligands by means of absorption, fluorescence lifetime, and ab initio molecular orbital calculations.

2. Result and discussion

2.1. Free ligand

Properties of free **L0**–**L2** ligands in water were studied first. Fluorescence spectra of the ligands (λ_{ex}=316 nm) measured without cations at different pH are summarized in Figure S1 Supplementary data. All these ligands show almost no fluorescence at entire pH range (2–13), with the fluorescence quantum yield (φ_F)<0.002. Figure 1 plots the fluorescence intensity of the ligands versus pH, where the dotted lines denote the mole fraction distribution of the different species, which is calculated from the protonation constants determined by potentiometric measurements (Table 1). No fluorescence of the ligands at the entire pH range is explained by the protonation states of nitrogen atoms for polyamine and quinoline moieties, as shown in Scheme 2. At pH

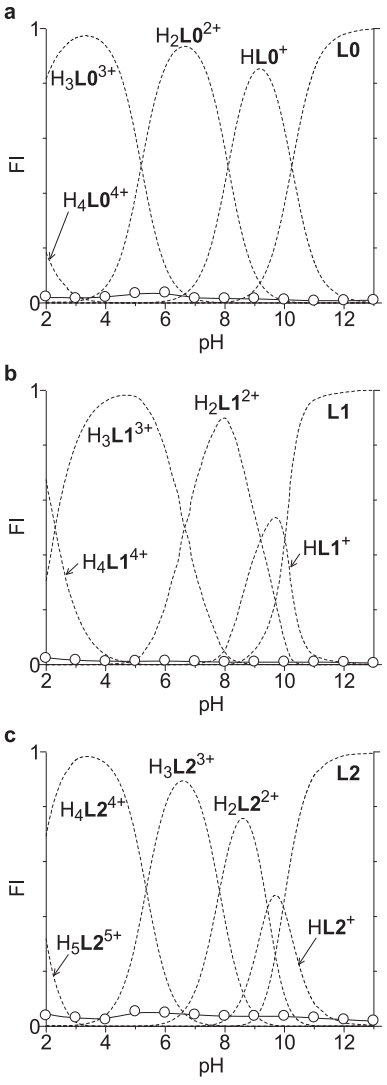

Figure 1. (Keys) pH-dependent change in fluorescence intensity (λ_{ex}=316 nm; 298 K) of (a) **L0** (λ_{em}=375 nm), (b) **L1** (λ_{em}=410 nm), and (c) **L2** (λ_{em}=410 nm) (50 μM) in an aqueous NaCl (0.15 M) solution measured without metal cations. (Lines) mole fraction distribution of the species. The fluorescence intensity (FI) of **L1** measured with 1 equiv of Zn^{2+} at pH 11 at 298 K (λ_{ex}=316 nm) is set as 1 (see Figs. 2 and 3). The fluorescence intensities of all figures in this manuscript are expressed as the relative intensity.

Table 1
Stepwise protonation constants of **L0**–**L2** determined in an aqueous NaCl (0.15 M) solution at 298 K

Reaction	log K		
	L0	L1	L2
$6H^+ + \mathbf{L} = H_6\mathbf{L}^{6+}$			
$5H^+ + \mathbf{L} = H_5\mathbf{L}^{5+}$			36.76±1.00
$4H^+ + \mathbf{L} = H_4\mathbf{L}^{4+}$		28.28±0.43	32.57±0.15
$3H^+ + \mathbf{L} = H_3\mathbf{L}^{3+}$	22.27±0.56	25.74±0.12	27.20±0.11
$2H^+ + \mathbf{L} = H_2\mathbf{L}^{2+}$	17.16±0.38	19.08±0.10	19.39±0.07
$H^+ + \mathbf{L} = H\mathbf{L}^{+}$	9.16±0.31	9.91±0.11	9.96±0.09

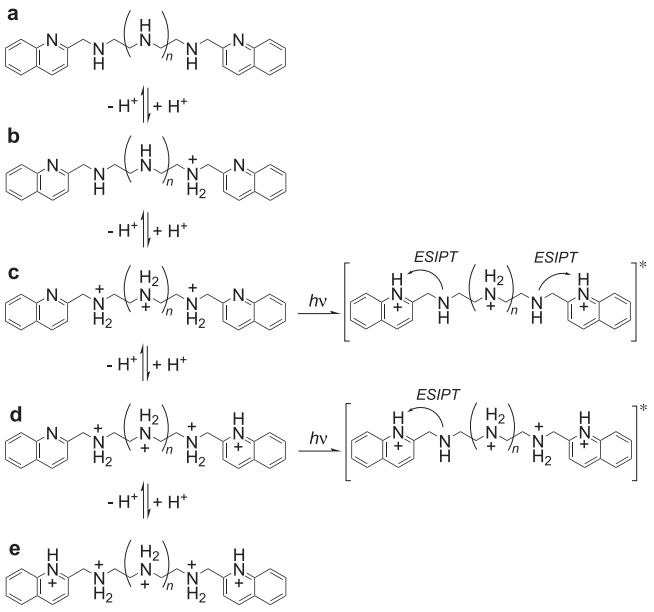

Scheme 2. Protonation/deprotonation sequence of **L0**–**L2**.

10–13, fully deprotonated species exist predominantly (Scheme 2a), whereas, partially protonated species exist mainly at pH 6–10 (Scheme 2b). These species undergo photoinduced electron transfer (PET) from the deprotonated polyamine nitrogens to the photoexcited quinoline fragments, resulting in fluorescence quenching.[11,12]

The fluorescence quenching of the ligands by the PET mechanism is confirmed by ab initio calculation with the Gaussian 03 program[13] using the time-dependent density functional theory (TDDFT) with the B3LYP/6-31+G(d) basis set. Table 2 shows the interfacial plots of key molecular orbitals of the fully deprotonated **L0**–**L2** species. As summarized in Table 3, the dominant orbital transitions of **L0** and **L2** are HOMO→LUMO, and that of **L1** is HOMO→LUMO+1, respectively. As shown in Table 2, the electron densities of LUMO and LUMO+1 orbitals for all of the ligands are located on the quinoline moieties, indicating that these orbitals have a π^* electronic character. In contrast, the electron densities of HOMO orbital for all of the ligands are located on the lone pair electrons on the nitrogen atoms of polyamine chains, where π orbitals of the quinoline moieties exist at lower energy level orbitals than HOMO−1. This clearly indicates that PET from the polyamine nitrogens to the excited quinoline fragments indeed occurs in these systems.[14] This thus results in fluorescence quenching of fully deprotonated or partially protonated **L0**–**L2** species.

At pH 4–6, all polyamine nitrogens of **L0**–**L2** are protonated (Scheme 2c) and, at pH 2–4, all polyamine nitrogens and one of the quinoline nitrogens are protonated (Scheme 2d). These species, however, still do not show fluorescence. This is due to the excited state intramolecular proton transfer (ESIPT) from the protonated polyamine nitrogens to the unprotonated quinoline fragments

Table 2
Interface plots of some molecular orbitals of fully deprotonated **L0**–**L2** species[a,b]

	L0	L1	L2
LUMO+1	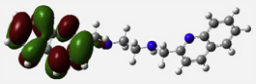	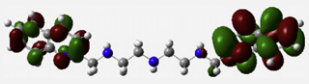	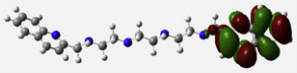
LUMO	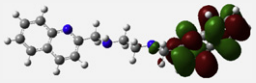	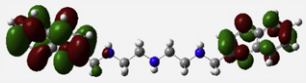	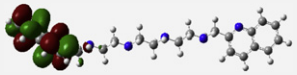
HOMO	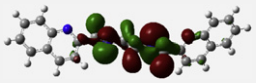	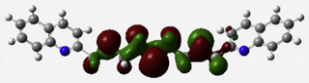	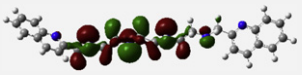
HOMO−1	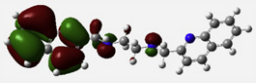	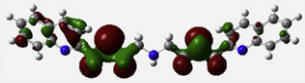	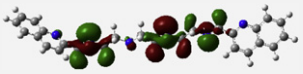
HOMO−2	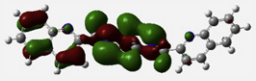	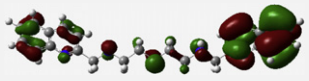	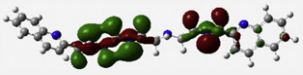

[a] Gray and blue atoms of the molecular framework indicate the carbon and nitrogen atoms.
[b] Green and deep red parts on HOMO and LUMO orbitals refer to the different phases of the molecular wave functions, where the isovalue is 0.02 a.u.

Table 3
Excitation energies (E) and oscillator strength (f) for the lowest excited singlet states of fully deprotonated **L0**–**L2** species obtained by TDDFT calculation

	Main orbital transition	CIC[a]	E (eV)	f
L0	HOMO−2→LUMO	−0.20498	3.9004	0.0131
	HOMO→LUMO	0.65171		
L1	HOMO−1→LUMO+1	−0.32254	4.0453	0.0313
	HOMO→LUMO	0.27986		
	HOMO→LUMO+1	0.47417		
L2	HOMO−2→LUMO	−0.22955	3.8751	0.0088
	HOMO−1→LUMO	−0.40451		
	HOMO→LUMO	0.50760		

[a] CI expansion coefficients for the main orbital transitions.

(Scheme 2c and d).[15] This leads to a PET from the resulting deprotonated polyamine nitrogens to the photoexcited quinoline fragments and, hence, results in fluorescence quenching. As a result of this, **L0**–**L2** ligands do not show fluorescence without metal cations at the entire pH range 2–13 (Fig. 1).

2.2. Effect of Zn(II)

Effects of Zn^{2+} addition on the fluorescence properties of **L0**–**L2** were studied. Figure 2 shows the pH-dependent change in fluorescence spectra of the ligands measured with 1 equiv of Zn^{2+}. The Zn^{2+} addition creates a strong fluorescence at 320–560 nm. Figure 3 shows the change in fluorescence intensity monitored at the maximum emission wavelengths, where the dotted lines denote the mole fraction distribution of the species, which were calculated from the protonation and stability constants determined potentiometrically (Tables 1 and 4). For all ligands, the fluorescence intensity is almost zero at pH<4, where Zn^{2+}-free species exist. In contrast, at pH>4, a large fluorescence enhancement is observed, which is consistent with the coordination of the ligands with Zn^{2+}.

The emission appearance of the ligands upon coordination with Zn^{2+} is due to the decrease in electron density of the polyamine nitrogens, leading to a suppression of PET from the polyamine nitrogens to the excited state quinoline fragments.[11,12] This is confirmed by ab initio calculations. As shown in Table 5, the dominant orbital transitions of the Zn^{2+} complexes for all ligands are HOMO→LUMO and HOMO−1→LUMO. As shown in Table 6, the electronic clouds of the HOMO, HOMO−1, and LUMO orbitals are

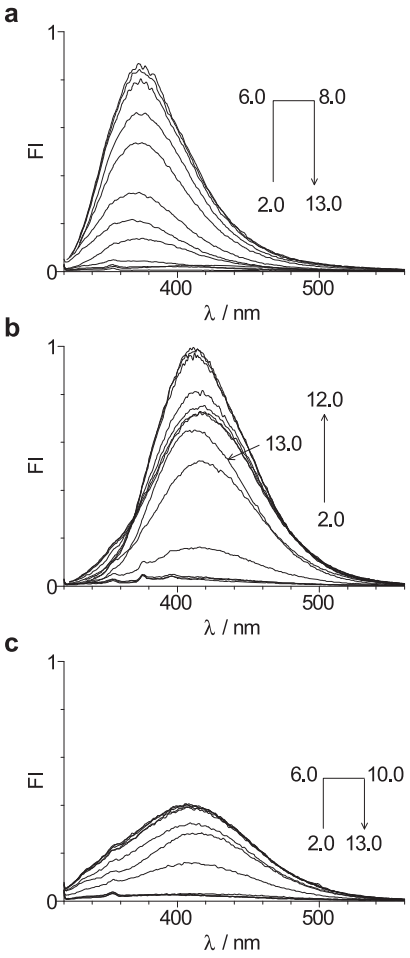

Figure 2. pH-dependent change in fluorescence spectra (λ_{ex}=316 nm; 298 K) of (a) **L0**, (b) **L1**, and (c) **L2** (50 μM) in an aqueous NaCl (0.15 M) solution measured with 1 equiv of $ZnCl_2$. The numbers in the figure denote pH of the solutions.

located on the quinoline moiety, indicating that the electronic transition has a π,π* character, where no electron density is located on the polyamine chain of the HOMO and HOMO−1 orbital. This suggests that the energy level of lone pair nitrogen of the

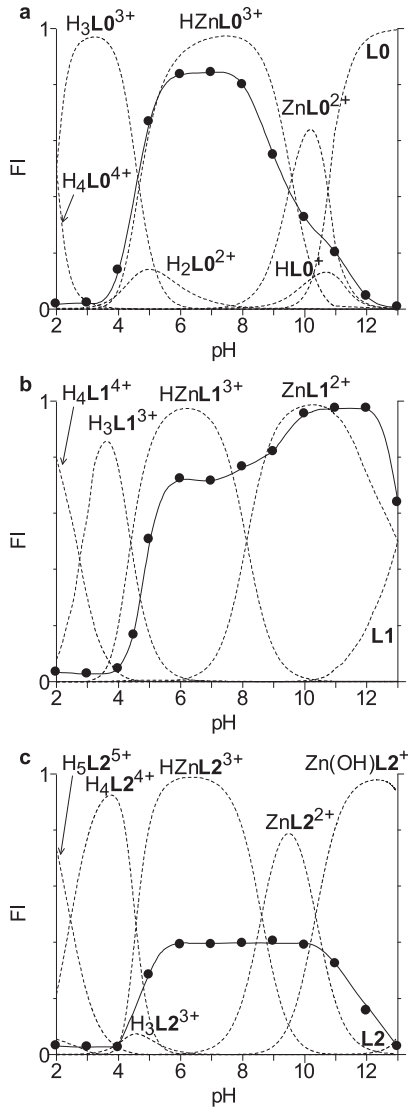

Figure 3. (Keys) pH-dependent change in fluorescence intensity (λ_{ex}=316 nm; 298 K) of (a) **L0** (λ_{em}=375 nm), (b) **L1** (λ_{em}=410 nm), and (c) **L2** (λ_{em}=410 nm) (50 μM) in an aqueous NaCl (0.15 M) solution measured with 1 equiv of $ZnCl_2$. (Lines) mole fraction distribution of the species. The mole fraction distribution of the Zn^{2+}-containing species is shown in Figure S2 Supplementary data.

Table 4
Stability constants for coordination between **L0**–**L2** and 1 equiv of $ZnCl_2$ in an aqueous NaCl (0.15 M) solution at 298 K

Reaction	log K		
	L0	L1	L2
$Zn^{2+}+HL^{+}=HZnL^{3+}$	8.38±0.46	11.48±0.22	12.63±0.23
$Zn^{2+}+L=ZnL^{2+}$	8.12±0.22	13.14±0.13	13.97±0.16
$Zn^{2+}+OH^{-}+L=Zn(OH)L^{+}$			3.62±0.23

Table 5
Excitation energies (E) and oscillator strength (f) for the lowest excited singlet state of Zn^{2+} complexes obtained by TDDFT calculation

Species	Main orbital transition	CIC[a]	E (eV)	f
$HZnL0^{3+}$	HOMO→LUMO	0.70476	2.7142	0.0011
$ZnL0^{2+}$	HOMO−1→LUMO	0.44386	3.7418	0.0548
$HZnL1^{3+}$	HOMO→LUMO	0.70338	3.0082	0.0015
$ZnL1^{2+}$	HOMO→LUMO	0.70574	3.7217	0.0004
$HZnL2^{3+}$	HOMO→LUMO	0.70611	2.5553	0.0022
$ZnL2^{2+}$	HOMO→LUMO	0.70627	3.0777	0.0001
$Zn(OH)L2^{+}$	HOMO→LUMO	0.57281	4.0983	0.0040

[a] CI expansion coefficients for the main orbital transitions.

Table 6
Interface plots of the key molecular orbitals for Zn^{2+} complexes[a,b]

Optimized structure	Molecular orbitals	
$HZnL0^{3+}$	HOMO	LUMO
$ZnL0^{2+}$	HOMO–1	LUMO
$HZnL1^{3+}$	HOMO	LUMO
$ZnL1^{2+}$	HOMO	LUMO
$HZnL2^{3+}$	HOMO	LUMO
$ZnL2^{2+}$	HOMO	LUMO
$Zn(OH)L2^{+}$	HOMO	LUMO

[a] Gray, blue, orange, and red atoms of the molecular framework indicate the carbon, nitrogen, zinc, and oxygen atoms.
[b] Green and deep red parts on HOMO and LUMO orbitals refer to the different phases of the molecular wave functions, where the isovalue is 0.02 a.u.

polyamine chain becomes lower than that of the quinoline π electrons upon Zn^{2+} coordination.[14] This thus suppresses the PET quenching process and allows fluorescence appearance.

As shown in Figure 3, Zn^{2+} complexes for all ligands have two emitting species, such as $HZnL^{3+}$ formed at ca. pH 7 and ZnL^{2+} formed at ca. pH 10. These species, however, show different fluorescence behaviors. In the case of **L0** (Fig. 3a), $HZnL0^{3+}$ formed at ca.

pH 7 shows a strong fluorescence, but the intensity of Zn**L0**$^{2+}$ formed at ca. pH 10 is much lower. In contrast, for **L1** (Fig. 3b), HZn**L1**$^{3+}$ shows a fluorescence intensity lower than Zn**L1**$^{2+}$. In the case of **L2** (Fig. 3c), HZn**L2**$^{3+}$ and Zn**L2**$^{2+}$ species show similar fluorescence intensity. These data indicate that **L1** shows fluorescence enhancement at the widest pH range, 6–12. Table 7 summarizes the fluorescence quantum yield (φ_F) of the respective species measured at pH 7 and 10. The φ_F values of HZn**L**$^{3+}$ species (pH 7) for all ligands are similar (0.02–0.03). In contrast, at pH 10, Zn**L1**$^{2+}$ has a higher φ_F value (0.04) than the other Zn**L**$^{2+}$ species (0.02).

Table 7
Quantum yield[a] (ϕ_F) and fluorescence decay times[b] (τ) of the respective species

	HZn**L0**$^{3+}$ (pH 7)	Zn**L0**$^{2+}$ (pH 10)	HZn**L1**$^{3+}$ (pH 7)	Zn**L1**$^{2+}$ (pH 10)	HZn**L2**$^{3+}$ (pH 7)	Zn**L2**$^{2+}$ (pH 10)
ϕ_F	0.031	0.015	0.028	0.041	0.020	0.018
τ	0.8	0.8	9.2	14.2	4.3	4.2
χ^2	2.43	1.84	1.45	2.10	1.57	2.25

[a] determined with a standard quinine (30 μM) in 0.1 N H_2SO_4 (ϕ_F=0.55).
[b] The measurements were carried out with 1 equiv $ZnCl_2$ in an aqueous NaCl (0.15 M) solution at different pH (λ_{ex}=316 nm, 298 K). The detailed decay profiles are shown in Figure S3 Supplementary data.

As shown in Figure 3, the fluorescence intensity for all ligands decreases at pH>12. In the case of **L0** and **L1**, as shown in Figure S2 Supplementary data, a hydration of Zn^{2+} occurs at pH>12, forming Zn hydroxide species, such as $Zn(OH)_2$, $Zn(OH)_3^-$, and $Zn(OH)_4^{2-}$. This leads to a removal of Zn^{2+} from the ligands and, hence, results in fluorescence quenching. In the case of **L2**, the Zn^{2+} removal from the complex does not occur. However, in this case, a hydroxide anion (OH^-) coordinates to the Zn^{2+} center of the complex, with the formation of Zn(OH)**L2**$^+$ species (Fig. 3c). This leads to a fluorescence quenching by PET from the OH^- group to the photoexcited quinoline moiety.[16] As shown in Tables 5 and 6, electron density of HOMO orbital for the Zn(OH)**L2**$^+$ species is located on the OH^- group attached to the Zn^{2+} center, while that for the Zn**L2**$^{2+}$ species is located on the quinoline moiety. This clearly indicates that the PET from OH^- to the excited quinoline quenches the Zn(OH)**L2**$^+$ fluorescence.

2.3. Quantitative detection

Fluorescence response of **L0**–**L2** to the Zn^{2+} amount was studied. Figure 4 shows the change in fluorescence intensity with the Zn^{2+} amount. In the case of **L2** (Fig. 4c), stepwise Zn^{2+} addition leads to a linear increase in the fluorescence intensity at both pH 7 and 10, and the increase is saturated upon addition of 1 equiv of Zn^{2+}, as is the case for **L1** (Fig. 4b). This indicates that **L1** and **L2** strongly coordinate with Zn^{2+}. As shown in Figure 4a, **L0** also shows a linear intensity increase with the Zn^{2+} amount at both pH 7 and 10, but the intensity increase is not saturated upon addition of 1 equiv of Zn^{2+}. As shown in Table 4, **L1** and **L2** have high stability constants for Zn^{2+} coordination; log*K* (HZn**L**/Zn·H**L**) >11.48 and log*K* (Zn**L**/Zn·**L**) >13.14. **L0**, however, has much lower values; log*K* (HZn**L**/Zn·H**L**)=8.38, log*K* (Zn**L**/Zn·**L**)=8.12. The low stability constants of **L0** therefore result in insufficient fluorescence response of **L0** to the Zn^{2+} amount. The results suggest that **L1** and **L2** enable quantification of Zn^{2+} in neutral–basic media, but **L0** does not.

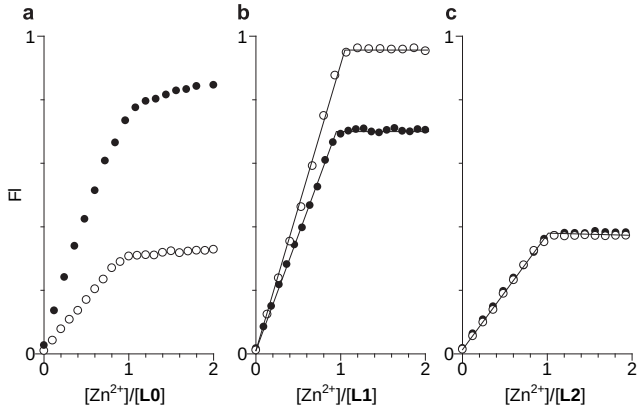

Figure 4. Change in fluorescence intensity (λ_{ex}=316 nm; 298 K) of (a) **L0** (λ_{em}=375 nm), (b) **L1** (λ_{em}=410 nm), and (c) **L2** (λ_{em}=410 nm) (50 μM) with the amount of Zn^{2+} added, (closed keys) at pH 7.0 (KH_2PO_4–NaOH buffer) and (open keys) at pH 10.0 ($NaHCO_3$–NaOH buffer). Change in fluorescence spectra is shown in Figure S4 Supplementary data.

2.4. Zn(II) selectivity

Fluorescence response of **L0**–**L2** to other metal cations was studied. As shown in Figure 5, addition of Zn^{2+} to **L0** and **L2** creates a large fluorescence enhancement, while most of other metal cations (Li^+, K^+, Mg^{2+}, Ca^{2+}, Fe^{3+}, Al^{3+}, Co^{2+}, Ni^{2+}, Cu^{2+}, Mn^{2+}, Hg^{2+}, Pb^{2+}, Ag^+) show almost no fluorescence, as does **L1**. The mechanism for almost no emission enhancement of **L0** and **L2** by these cations is probably similar to that of **L1**, as described previously.[11] It is well known that most of early reported Zn^{2+} probes show similar fluorescence enhancement against Cd^{2+}.[4,5c] As described previously[11] and shown in Figure 5b, the **L1** probe shows very low fluorescence enhancement against Cd^{2+}; the fluorescence intensity obtained with Zn^{2+} is more than 7-fold of that obtained with Cd^{2+}

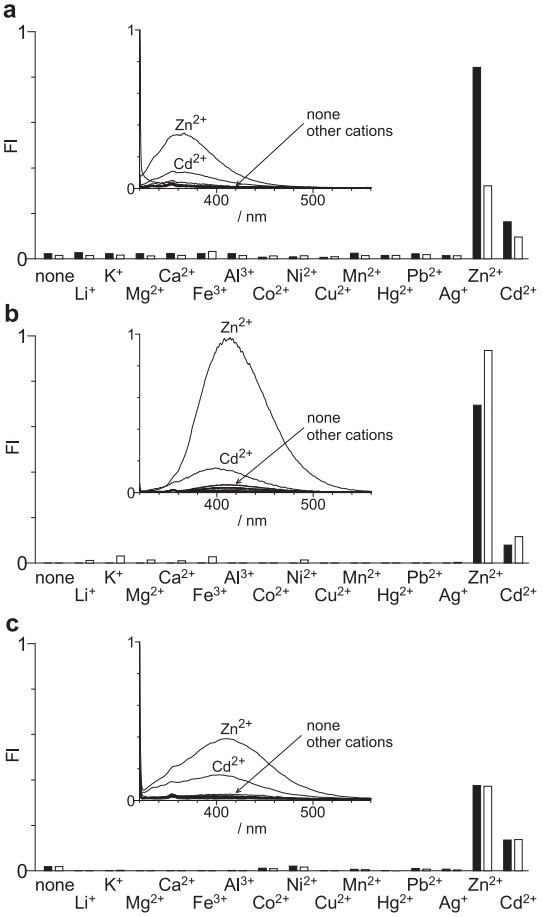

Figure 5. Fluorescence intensity (λ_{ex}=316 nm; 298 K) of (a) **L0** (λ_{em}=375 nm), (b) **L1** (λ_{em}=410 nm), and (c) **L2** (λ_{em}=410 nm) (50 μM) measured with 1 equiv of respective metal cations, (black bar) at pH 7.0 (KH_2PO_4–NaOH buffer) and (white bar) pH 10.0 ($NaHCO_3$–NaOH buffer). (Inset) Fluorescence spectra obtained at pH 10.0. The spectra obtained at pH 7.0 are shown in Figure S5 Supplementary data.

at both pH 7 and 10. However, as shown in Figure 5a and c, the intensity of **L0** and **L2** obtained with Zn^{2+} is less than 5-fold of that obtained with Cd^{2+} at both pH 7 and 10. This indicates that **L1** shows the most selective emission enhancement against Zn^{2+}.

Further experiments were conducted to see the effects competing cations on the **L1** fluorescence. Figure 6a shows the fluorescence intensity of **L1** when measured at pH 10 with 1 equiv of Zn^{2+} together with 1 equiv of each other cation. The Zn^{2+}-induced fluorescence enhancement is scarcely affected by Li^{+}, K^{+}, Mg^{2+}, Ca^{2+}, Fe^{3+}, Al^{3+}, Mn^{2+}, and Pb^{2+}. In contrast, other transition metal cations, such as Co^{2+}, Ni^{2+}, Cu^{2+}, Hg^{2+}, Ag^{+}, and Cd^{2+}, strongly quench the fluorescence. This indicates that these cations coordinate more strongly with **L1**. Figure 6b shows the fluorescence intensity of **L1** measured with 0.5 equiv of Zn^{2+} together with 0.5 equiv of each other cation. In this case, sufficient amount of **L1** for Zn^{2+} coordination exists; therefore, other cations do not affect the Zn^{2+}-induced fluorescence enhancement. As shown in Figure S6 Supplementary data, similar results are obtained at pH 7. The result indicates that addition of excess amount of **L1** enables selective detection of Zn^{2+} even in the presence of competing cations.

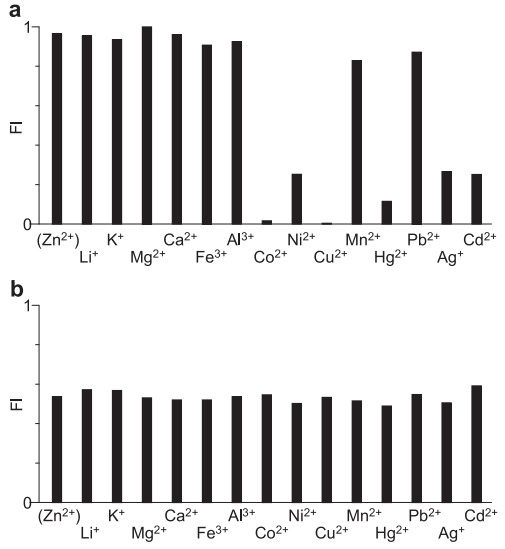

Figure 6. Fluorescence intensity (λ_{ex}=316 nm; 298 K) of **L1** (50 μM) monitored at λ_{em}=410 nm at pH 10 ($NaHCO_3$–NaOH buffer), when measured with (a) 1 equiv of $ZnCl_2$ together with 1 equiv of each other cation and (b) 0.5 equiv of $ZnCl_2$ together with 0.5 equiv of each other cation. The change in ^1H NMR spectra upon addition of Zn^{2+} and/or Cd^{2+} is shown in Figure S7 Supplementary data.

2.5. Emission wavelength

The emission wavelength of the Zn^{2+} complexes of **L0**–**L2** also depend on the polyamine chain length. As shown in Figure 2b and c, fluorescence spectra of **L1** and **L2** obtained with Zn^{2+} shows a maximum intensity at 410–420 nm. This is assigned to the emission from the π,π* excited state of quinoline, as observed for many quinoline derivatives.[17] In contrast, as shown in Figure 2a, **L0** shows a blue-shifted emission at 370–380 nm. As shown in Figure S8 Supplementary data, addition of excess amount of proton (5 M $HClO_4$) to the solution containing the respective **L0**–**L2** ligands shows a quinoline fluorescence at 420 nm. In that, the protonation of all polyamine and quinoline nitrogens suppresses the ESIPT and PET quenching processes and allows fluorescence appearance. The spectra are similar to the spectra of **L1** and **L2** obtained with Zn^{2+}. This indicates that the blue-shifted fluorescence of **L0** is due to the coordination with Zn^{2+}.

Table 7 shows the fluorescence lifetime of Zn^{2+} complexes. The lifetimes of the **L0** complexes are very short (0.8 ns) as compared to those of **L1** and **L2** complexes (4.2–14.2 ns), indicating that the excited state **L0** complexes are unstable. As shown in Table 6, the electronic excitation of the **L1** and **L2** complexes is a π,π* transition of the quinoline moiety, where no electron density is extended to the Zn^{2+} center both on HOMO and LUMO orbitals. In contrast, for **L0** complexes, the excitation is also a π,π* transition, but π electron of the quinoline moiety in the LUMO orbital is extended to the Zn^{2+} center, where the electron density extension to Zn^{2+} is not observed on HOMO or HOMO−1 orbitals. This indicates that the electronic excitation of the **L0** complexes probably involves a partial charge transfer from the quinoline moiety to the Zn^{2+} center. However, as shown in Figures S9 and S10 Supplementary data, absorption spectra of the **L0** complexes are similar to that of free **L0**. In addition, absorption and excitation spectra of the **L0** complexes are similar to those of the **L1** and **L2** complexes (Fig. S11, Supplementary data). These findings suggest that the partial charge transfer of the **L0** complexes occurs in the excited state,[18] and this probably leads to a fluorescence blue shift of the **L0** complexes.

The excited state charge transfer is probably due to the steric tightness of the **L0** complexes. As reported,[19] the charge transfer transition energy generally increases with a decrease in the distance between the metal cation and the ligand atom and, hence, results in a fluorescence blue shift. As shown in Table 8, the distances between quinoline nitrogens and Zn^{2+} for the **L0** complexes are determined by ab initio calculation to be 2.002–2.066 Å. In contrast, the distances of **L1** and **L2** complexes are 2.062–2.179 Å and 2.098–2.112 Å, respectively. This suggests that the **L0** complexes indeed have relatively shorter Zn–N distances than the **L1** and **L2** complexes. The shorter Zn–N distance of the **L0** complexes probably leads to a blue shift of the fluorescence.

Table 8
The distance (Å) between Zn^{2+} and quinoline nitrogens (Q1, Q2) or polyamine nitrogens (A1–A4) of the Zn^{2+} complexes determined by ab initio calculation[a]

	$HZnL0^{3+}$	$ZnL0^{2+}$	$HZnL1^{3+}$	$ZnL1^{2+}$	$HZnL2^{3+}$	$ZnL2^{2+}$
$Zn^{2+}\cdots$Q1	2.035	2.066	2.099	2.179	2.112	2.098
$Zn^{2+}\cdots$Q2	2.002	2.065	2.062	2.115	3.835	3.850
$Zn^{2+}\cdots$A1	3.572 (protonated)	2.129	3.816 (protonated)	2.183	3.872 (protonated)	3.208
$Zn^{2+}\cdots$A2	2.186	2.178	2.226	2.310	2.200	2.120
$Zn^{2+}\cdots$A3			2.138	2.168	2.143	2.204
$Zn^{2+}\cdots$A4					2.127	2.143

[a] The positions of the nitrogen atoms for the respective complexes are indicated in Table 6.

3. Conclusions

Coordination and fluorescence properties of polyamines bearing two terminal quinoline fragments, **L0**, **L1**, and **L2**, have been studied in water. Without cations, these ligands show no fluorescence at entire pH range, but addition of Zn^{2+} leads to strong fluorescence enhancement at pH>4. For all ligands, mono- or nonprotonated $HZnL^{3+}$ and ZnL^{2+} species behave as emission components; however, their emission properties depend strongly on the polyamine chain length. Coordination of **L1** or **L2** with Zn^{2+} is strong and shows linear and stoichiometrical response to the Zn^{2+} amount, while **L0** shows insufficient response due to low binding constants. The emission selectivity of **L0** and **L2** for Zn^{2+} is lower than that of **L1**; they show relatively strong fluorescence against Cd^{2+}. The Zn^{2+} complexes of **L1** and **L2** show fluorescence at 410 nm derived from π,π* transition of quinoline, while the complexes of **L0** show a blue-shifted emission at 375 nm. Ab initio calculation revealed that the emission blue shift is derived from the partial charge transfer process from the excited state quinoline moieties to Zn^{2+}.

4. Experimental

4.1. Materials

All reagents used were supplied from Wako and Tokyo Kasei and used without further purification. Water was purified by the Milli Q system. **L1** was synthesized according to a procedure described previously.[11] **L0** and **L2** were synthesized as follows:

Compound **L0**. 2-Quinolinecarbaldehyde (0.47 g, 3.0 mmol) and ethylenediamine (0.09 g, 1.5 mmol) were stirred in EtOH (50 mL) at 298 K for 17 h under dry N_2. $NaBH_4$ (1.03 g, 27 mmol) was added to the solution and stirred at 323 K for 4 h. The resultant was concentrated by evaporation, and water (30 mL) was added to the residue. The solution was extracted with CH_2Cl_2 (30 mL×3), and the combined organic layer was dried over Na_2SO_4 and concentrated by evaporation. The residue was dissolved in EtOH and precipitated by an addition of HCl, affording a beige powder of **L0** as a HCl salt (0.45 g, yield: 72 %). ^{1}H NMR (270 MHz, DMSO-d_6, TMS): δ=3.65 (s, 4H, CH_2 of polyamine), 4.65 (s, 4H, ArCH_2), 7.65–8.51 (m, 12H, ArH). ^{13}C NMR (68 MHz, DMSO-d_6, TMS): δ=152.33, 146.08, 137.16, 129.99, 127.96, 127.83, 126.96, 126.77, 120.18, 50.53, 43.20. FAB-MS: calcd for $C_{22}H_{22}N_4$: 342.18. Found: m/z 343.2 (M+H$^+$). HRMS (FAB$^+$): calcd for $C_{22}H_{23}N_4$ [M+H$^+$]: 343.1923. Found: m/z 343.1931 (M+H$^+$). ^{1}H, ^{13}C NMR and FAB-MS charts are shown in Figures S12–S14.

Compound **L2**. This was synthesized in a manner similar to **L0** with 2-quinolinecarbaldehyde (0.47 g, 3.0 mmol) and triethylenetetramine (0.22 g, 1.5 mmol), as a beige powder of **L2** as a HCl salt (0.60 g, yield: 69 %). ^{1}H NMR (270 MHz, DMSO-d_6, TMS): δ=3.28–3.55 (m, 12H, CH_2 of polyamine), 4.65 (s, 4H, ArCH_2), 7.64–8.50 (m, 12H, ArH). ^{13}C NMR (100 MHz, DMSO-d_6, TMS): δ=152.34, 146.19, 137.17, 130.04, 128.10, 127.87, 127.00, 126.81, 120.13, 50.58, 42.84, 42.62,42.25. FAB-MS: calcd for $C_{26}H_{32}N_6$: 428.27. Found: m/z 429.3 (M+H$^+$). HRMS (FAB$^+$): calcd for $C_{26}H_{33}N_6$ [M+H$^+$]: 429.2767. Found: m/z 429.2754 (M+H$^+$). ^{1}H, ^{13}C NMR and FAB-MS charts are shown in Figures S15–S17.

4.2. Spectroscopic measurements

Steady-state fluorescence spectra were measured on a Hitachi F-4500 fluorescence spectrophotometer.[20] The spectra were measured at 298±1 K using a 10 mm path length quartz cell. Absorption spectra were measured on an UV–visible photodiode-array spectrophotometer (Shimadzu; Multispec-1500) at 298±1 K. Fluorescence lifetime was measured on a PTI-3000 apparatus (Photon Technology International) at 298±1 K using a Xe nanoflash lamp filled with N_2.[21] All measurements were carried out with NaCl to maintain the ionic strength of the solution (I=0.15 M). Metal salts used were LiCl, KCl, $CaCl_2$, $MgCl_2$, $CoCl_2$, $NiCl_2$, $FeCl_3$, $CuCl_2$, $ZnCl_2$, $CdCl_2$, $HgCl_2$, $AlCl_3$, $Pb(NO_3)_2$, and $AgNO_3$, respectively. All measurements were carried out in an aerated condition. ^{1}H and ^{13}C NMR spectra were obtained by a JEOL JNM-GSX270 Excalibur. FAB-MS spectra were obtained by a JEOL JMS-700 Mass Spectrometer.

4.3. Potentiometric titrations

This was performed on a COMTITE-550 potentiometric automatic titrator (Hiranuma Co, Ltd.) with a glass electrode GE-101.[20] Aqueous solution (50 mL) containing respective ligand (0.027 mmol) with or without metal cation was kept under dry nitrogen with an ionic strength of I=0.15 M (NaCl) at 298 K. The titration was done at 298±1 K using an aqueous NaOH (4.3 mM) solution. The program HYPERQUAD was employed for determination of the protonation and stability constants.[22] K_w (=[H$^+$][OH$^-$]) value used is $10^{-14.00}$ (298 K). The stability constants used for Zn hydroxide (298 K) were log$K$ (Zn(OH)/Zn·OH)=−9.21, log$K$ (Zn(OH)$_2$/Zn·2OH)=−17.14, log$K$ (Zn(OH)$_3$/Zn·3OH)=−28.4, log$K$ (Zn(OH)$_4$/Zn·4OH)=−40.71, log$K$ (Zn$_2$(OH)/2Zn·OH)=−8.75, and log$K$ (Zn$_2$(OH)$_6$/2Zn·6OH)=−57.55, respectively.[23]

4.4. Computational details

Ab initio calculations were performed with the Gaussian 03 program.[13] Geometry optimization was carried out with the density functional theory (DFT) using the B3LYP function. Metal-free compounds were calculated using the 6-31G(+d) basis set. Zn^{2+} complexes were calculated using the LANL2DZ basis set. The electronic excitation energies and oscillator strengths were calculated with the time-dependent density functional theory (TDDFT).

Acknowledgements

This work was supported by the Grant-in-Aid for Scientific Research (No. 21760619) from the Ministry of Education, Culture, Sports, Science and Technology, Japan (MEXT). C.I. thanks the Global COE Program 'Global Education and Research Center for Bio-Environmental Chemistry' of Osaka University.

Supplementary data

The data contains Figures S1–S17 and Cartesian coordinates for compounds. Supplementary data associated with this article can be found in the online version, at doi:10.1016/j.tet.2010.05.096. These data include MOL files and InChiKeys of the most important compounds described in this article.

References and notes

1. Vallee, B. L.; Falchuk, K. H. *Physiol. Rev.* **1993**, *73*, 79–118.
2. (a) Czarnik, A. W. *Fluorescent Chemosensors of Ion and Molecule Recognition*; American Chemical Society: Washington, DC, 1993; (b) de Silva, A. P.; Gunaratne, H. Q. N.; Gunnlaugsson, T.; Huxley, A. J. M.; McCoy, C. P.; Rademacher, J. T.; Rice, T. E. *Chem. Rev.* **1997**, *97*, 1515–1566; (c) Valeur, B.; Leray, I. *Coord. Chem. Rev.* **2000**, *205*, 3–40; (d) Prodi, L.; Bolletta, F.; Montalti, M.; Zaccheroni, N. *Coord. Chem. Rev.* **2000**, *205*, 59–83; (e) Jiang, P.; Guo, Z. *Coord. Chem. Rev.* **2004**, *248*, 205–229; (f) Carol, P.; Sreejith, S.; Ajayaghosh, A. *Chem.—Asian J.* **2007**, *2*, 338–348; (g) Dai, Z.; Canary, J. W. *New J. Chem.* **2007**, *31*, 1708–1718.
3. (a) Hirano, T.; Kikuchi, K.; Urano, Y.; Higuchi, T.; Nagano, T. *J. Am. Chem. Soc.* **2000**, *122*, 12399–12400; (b) Nolan, E. M.; Jaworski, J.; Okamoto, K.-i.; Hayashi, Y.; Sheng, M.; Lippard, S. J. *J. Am. Chem. Soc.* **2005**, *127*, 16812–16823; (c) Zhang, X.-a.; Hayes, D.; Smith, S. J.; Friedle, S.; Lippard, S. J. *J. Am. Chem. Soc.* **2008**, *130*, 15788–15789; (d) Komatsu, K.; Kikuchi, K.; Kojima, H.; Urano, Y.; Nagano, T. *J. Am. Chem. Soc.* **2005**, *127*, 10197–10204; (e) Nolan, E. M.; Jaworski, J.; Racine, M. E.; Sheng, M.; Lippard, S. J. *Inorg. Chem.* **2006**, *45*, 9748–9757.
4. (a) Lim, N. C.; Schuster, J. V.; Porto, M. C.; Tanudra, M. A.; Yao, L.; Freake, H. C.; Brückner, C. *Inorg. Chem.* **2005**, *44*, 2018–2030; (b) Lim, N. C.; Brückner, C. *Chem. Commun.* **2004**, 1094–1095; (c) Komatsu, K.; Urano, Y.; Kojima, H.; Nagano, T. *J. Am. Chem. Soc.* **2007**, *129*, 13447–13454.
5. (a) Jiang, P.; Chen, L.; Lin, J.; Liu, Q.; Ding, J.; Gao, X.; Gao, Z. *Chem. Commun.* **2002**, 1424–1425; (b) Koike, T.; Watanabe, T.; Aoki, S.; Kimura, E.; Shiro, M. *J. Am. Chem. Soc.* **1996**, *118*, 12696–12703; (c) Kim, T. W.; Park, J.-h.; Hong, J.-I. *J. Chem. Soc., Perkin Trans. 2* **2002**, 923–927; (d) O'Connor, N. A.; Sakata, S. T.; Zhu, H.; Shea, K. J. *Org. Lett.* **2006**, *8*, 1581–1584.
6. (a) Turfan, B.; Akkaya, E. U. *Org. Lett.* **2002**, *4*, 2857–2859; (b) Harriman, A.; Mallon, L. J.; Stewart, B.; Ulrich, G.; Ziessel, R. *Eur. J. Org. Chem.* **2007**, 3191–3198; (c) Atilgan, S.; Ozdemir, T.; Akkaya, E. U. *Org. Lett.* **2008**, *10*, 4065–4067.
7. (a) Fahrni, C. J.; O'Halloran, T. V. *J. Am. Chem. Soc.* **1999**, *121*, 11448–11458; (b) Zhang, Y.; Guo, X.; Si, W.; Jia, L.; Qian, X. *Org. Lett.* **2008**, *10*, 473–476; (c) Royzen, M.; Durandin, A.; Young, V. C., Jr.; Geacintov, N. E.; Canary, J. W. *J. Am. Chem. Soc.* **2006**, *128*, 3854–3855; (d) Mikata, Y.; Yamanaka, A.; Yamashita, A.; Yano, S. *Inorg. Chem.* **2008**, *47*, 7295–7301; (e) Mikata, Y.; Wakamatsu, M.; Yano, S. *Dalton Trans.* **2005**, 545–550; (f) Gan, W.; Jones, S. B.; Reibenspies, J. H.; Hancock, R. D. *Inorg. Chim. Acta* **2005**, *358*, 3958–3966; (g) Mameli, M.; Aragon, M. C.; Arca, M.; Atzor, M.; Bencini, A.; Bazzicalupi, C.; Blake, A. J.; Caltagirone, C.; Devillanova, F. A.; Garau, A.; Hursthouse, M. B.; Isaia, F.; Lippolis, V.; Valtancoli, B. *Inorg. Chem.* **2009**, *48*, 9236–9246.
8. Lim, N. C.; Freake, H. C.; Brückner, C. *Chem.—Eur. J.* **2005**, *11*, 38–49.
9. Yin, Q.; Zhang, Z.; Zhao, Y.-F. *J. Chem. Res.* **2006**, 160–162.
10. (a) Aoki, S.; Sakurama, K.; Matsuo, N.; Yamada, Y.; Takasaka, R.; Tanuma, S.-i.; Shiro, M.; Takeda, K.; Kimura, E. *Chem.—Eur. J.* **2006**, *12*, 9066–9080; (b) Akkaya, E. U.; Huston, M. E.; Czarnik, A. W. *J. Am. Chem. Soc.* **1990**, *112*, 3590–3593;

(c) de Silva, S. A.; Zavaleta, A.; Baron, D. E. *Tetrahedron Lett.* **1997**, *38*, 2237–2240; (d) Castagnetto, J. M.; Canary, J. W. *Chem. Commun.* **1998**, 203–204.
11. Shiraishi, Y.; Ichimura, C.; Hirai, T. *Tetrahedron Lett.* **2007**, *48*, 7769–7773.
12. (a) Aldelda, M. T.; Díaz, P.; García-España, E.; Lima, J. C.; Lodeiro, C.; de Melo, J. S.; Palola, A. J.; Pina, F.; Soriano, C. *Chem. Phys. Lett.* **2002**, *353*, 63–68; (b) Parola, A. J.; Lima, J. C.; Pina, F.; Pina, J.; de Melo, J. S.; Soriano, C.; García-España, E.; Aucejo, R.; Alarcón, J. *Inorg. Chim. Acta* **2007**, *360*, 1200–1208; (c) Alves, S.; Pina, F.; Albelda, M. T.; García-España, E.; Soriano, C.; Luis, S. V. *Eur. J. Inorg. Chem.* **2001**, 405–412; (d) Sclafani, J. A.; Maranto, M. T.; Sisk, T. M.; Van Arman, S. A. *Tetrahedron Lett.* **1996**, *37*, 2193–2196.
13. Frisch, M. J.; Trucks, G. W.; Schlegel, H. B.; Scuseria, G. E.; Robb, M. A.; Cheeseman, J. R.; Montgomery, J. A.; Vreven, T., Jr.; Kudin, K. N.; Burant, J. C.; Millam, J. M.; Iyengar, S. S.; Tomasi, J.; Barone, V.; Mennucci, B.; Cossi, M.; Scalmani, G.; Rega, N.; Petersson, G. A.; Nakatsuji, H.; Hada, M.; Ehara, M.; Toyota, K.; Fukuda, R.; Hasegawa, J.; Ishida, M.; Nakajima, T.; Honda, Y.; Kitano, O.; Nakai, H.; Klene, M.; Li, X.; Knox, J. E.; Hratchian, H. P.; Cross, J. B.; Bakken, V.; Adamo, C.; Jaramillo, J.; Gomperts, R.; Stratmann, R. E.; Yazyev, O.; Austin, A. J.; Cammi, R.; Pomelli, C.; Ochterski, J.; Ayala, P. Y.; Morokuma, K.; Voth, G. A.; Salvador, P.; Dannenberg, J. J.; Zakrzewski, V. G.; Dapprich, S.; Daniels, A. D.; Strain, M. C.; Farkas, O.; Malick, D. K.; Rabuck, A. D.; Raghavachari, K.; Foresman, J. B.; Ortiz, J. V.; Cui, Q.; Baboul, A. G.; Clifford, S.; Cioslowski, J.; Stefanov, B. B.; Liu, G.; Liashenko, A.; Piskorz, P.; Komaromi, I.; Martin, R. L.; Fox, D. J.; Keith, T.; Al-Laham, M. A.; Peng, Y.; Nanayakkara, A.; Challacombe, M.; Gill, P. M. W.; Johnson, B. G.; Chen, W.; Wong, M. W.; Gonzalez, C.; Pople, J. A. *Gaussian 03, Revision B.05*; Gaussian: Pittsburgh, PA, 2003.
14. (a) Tal, S.; Salman, H.; Abraham, Y.; Botoshansky, M.; Eichen, Y. *Chem.—Eur. J.* **2006**, *12*, 4858–4874; (b) Salman, H.; Tal, S.; Chuvilov, Y.; Solovey, O.; Abraham, Y.; Kapon, M.; Suwinska, K.; Eichen, Y. *Inorg. Chem.* **2006**, *45*, 5315–5320.
15. (a) Kyrychenko, A.; Waluk, J. *J. Phys. Chem. A* **2006**, *110*, 11958–11967; (b) Schulman, S. G.; Sanders, L. B. *Anal. Chim. Acta* **1971**, *56*, 83–89; (c) Liu, Y.; Zhang, N.; Chen, Y.; Wang, L.-H. *Org. Lett.* **2007**, *9*, 315–318.
16. (a) Fabbrizzi, L.; Fravelli, I.; Francese, G.; Licchelli, M.; Perotti, A.; Taglietti, A. *Chem. Commun.* **1998**, 971–972; (b) Shiraishi, Y.; Kohno, Y.; Hirai, T. *J. Phys. Chem. B* **2005**, *109*, 19139–19147.
17. (a) Snyder, R.; Testa, A. C. *J. Phys. Chem.* **1984**, *88*, 5948–5950; (b) Kawakami, J.; Miyamoto, R.; Kimura, K.; Obata, K.; Nagaki, M.; Kitahara, H. *J. Comput. Chem. Jpn.* **2003**, *2*, 57–62; (c) Ou, S.; Lin, Z.; Duan, C.; Zhang, H.; Bai, Z. *Chem. Commun.* **2006**, 4392–4394.
18. Baruah, M.; Qin, W.; Flors, C.; Hofkens, J.; Vallee, R. A. L.; Beljonne, D.; Van der Auweraer, M.; De Borggreve, W. M.; Boens, N. *J. Phys. Chem. A.* **2006**, *110*, 5998–6009.
19. (a) Brik, M. G. *J. Phys. Chem. Solids* **2007**, *68*, 1341–1347; (b) Ando, K. *J. Phys. Chem. B* **2008**, *112*, 250–256.
20. (a) Shiraishi, Y.; Tokitoh, Y.; Nishimura, G.; Hirai, T. *Org. Lett.* **2005**, *7*, 2611–2614; (b) Shiraishi, Y.; Tokitoh, Y.; Hirai, T. *Chem. Commun.* **2005**, 5316–5318.
21. (a) Shiraishi, Y.; Tokitoh, Y.; Hirai, T. *Org. Lett.* **2006**, *8*, 3841–3844; (b) Shiraishi, Y.; Tokitoh, Y.; Nishimura, G.; Hirai, T. *J. Phys. Chem. B* **2007**, *111*, 5090–5100.
22. Sabatini, A.; Vacca, A.; Gans, P. *Coord. Chem. Rev.* **1992**, *120*, 389–405.
23. Baes, C. F.; Mesmer, R. E. *The Hydrolysis of Cations*; Wiley: New York, NY, 1976.